International Journal of Pharmaceutics 582 (2020) 119335

Contents lists available at ScienceDirect

International Journal of Pharmaceutics

journal homepage: www.elsevier.com/locate/ijpharm

Choline and amino acid based biocompatible ionic liquid mediated transdermal delivery of the sparingly soluble drug acyclovir

Md. Rafiqul Islam[a,b], Md. Raihan Chowdhury[a], Rie Wakabayashi[a,c], Yoshiro Tahara[a], Noriho Kamiya[a,c,d], Muhammad Moniruzzaman[e], Masahiro Goto[a,c,d,*]

[a] Department of Applied Chemistry, Graduate School of Engineering, Kyushu University, 744 Motooka, Nishi-ku, Fukuoka 819-0395, Japan
[b] Department of Applied Chemistry and Chemical Engineering, Noakhali Science and Technology University, Noakhali 3814, Bangladesh
[c] Advanced Transdermal Drug Delivery System Center, Kyushu University, 744 Motooka, Nishi-ku, Fukuoka 819-0395, Japan
[d] Division of Biotechnology, Center for Future Chemistry, Kyushu University, 744 Motooka, Nishi-ku, Fukuoka 819-0395, Japan
[e] Chemical Engineering Department, Universiti Teknologi PETRONAS, 32610 Seri Iskandar, Perak, Malaysia

ARTICLE INFO

Keywords:
Biocompatible
Ionic liquid
Transdermal drug delivery system
Acyclovir

ABSTRACT

Transdermal delivery of drugs is more challenging for drugs that are insoluble or sparingly soluble in water and most organic solvents. To overcome this problem, ionic liquid (IL)-mediated ternary systems have been suggested as potential drug carriers. Here, we report potent ternary (IL–EtOH–IPM) systems consisting of biocompatible ILs, ethanol (EtOH), and isopropyl myristate (IPM) that can dissolve a significant amount of the sparingly soluble drug acyclovir (ACV). The ternary systems were optically transparent and thermodynamically stable with a wide range of IL pertinence. An *in vitro* drug permeation study showed that the ILs in the ternary systems dramatically enhanced ACV permeation into and across the skin. Fourier Transform Infrared spectroscopy of the stratum corneum (sc) after treatment with ternary systems showed that the skin barrier function was reduced by disturbance of the regularly ordered arrangement of corneocytes and modification of the surface properties of the sc during permeation. Histological analysis, and skin irritation studies using a reconstructed human epidermis model showed the safety profile of the ternary system, and there were no significant changes in the structures of the sc, epidermis, and dermis. Therefore, ternary systems containing biocompatible ILs are promising for transdermal delivery of insoluble or sparingly soluble drugs.

1. Introduction

Transdermal drug delivery systems (TDDSs) have attracted much attention. TDDSs are safe and non-invasive drug administration systems that systematically deliver drug molecules across the skin. These systems offer some advantages over conventional therapeutic strategies (i.e., oral and injection), such as better patient compliance, reduced unwanted side effects, and avoiding first pass hepatic elimination (Amjadi et al., 2018; Prausnitz and Langer, 2008; Wu et al., 2019). However, TDDSs have some limitations for most drugs owing to the strong skin barrier function of the stratum corneum (sc, the outermost layer of the skin) (Carter et al., 2019; Szumała et al., 2019). To overcome this barrier function, various physical (iontophoresis, electroporation, and ultrasound) and chemical (prodrug, nanoparticle, and penetration enhancers) methods and their combination have been used to improve drug permeation (Chen et al., 2018; Karande and Mitragotri, 2009). Among these methods, chemical penetration enhancers are the most widely used method to augment permeation through the sc (Gupta et al., 2019; Lane, 2013; Monti et al., 2017). Despite the large number of identified chemical enhancers, very few have been taken to market because of the linear relation between the reinforcing effect and the toxicity in most of the cases (Chen et al., 2014; Gupta et al., 2019). It has been reported that combining two or more enhancers can stimulate drug permeation with reduced skin irritation (Arora et al., 2010; Liu et al., 2009). Several multicomponent aqueous systems (Kim et al., 2008; Watkinson et al., 2009) and

Abbreviations: ACV, Acyclovir; [Ch][AAs], Choline amino acids; [Ch][Gly], Choline glycinate; [Ch][Ser], Choline serinate; [Ch][Ala], Choline alaninate; [Ch][Cl], Choline chloride; [Ch][OH], Choline hydroxide; [Bmim][Cl], 1-Butyl-3-methylimidazolium imidazolium chloride; [C1mim][DMP], Dimethylimidazolium dimethylphosphate; EtOH, Ethanol, anhydrous; IL, Ionic liquid; IPM, Isopropyl myristate; SC, Stratum corneum; TDDS, Transdermal drug delivery system; YMP, Yucatan micropig; MEM, Gibco minimum essential media; D-PBS, Dulbecco's phosphate buffered saline; TS, Ternary system

* Corresponding author at: Graduate School of Engineering, Kyushu University, 744 Motooka, 819-0395 Fukuoka, Japan.
E-mail address: m-goto@mail.cstm.kyushu-u.ac.jp (M. Goto).

https://doi.org/10.1016/j.ijpharm.2020.119335
Received 9 January 2020; Received in revised form 28 March 2020; Accepted 12 April 2020
Available online 18 April 2020
0378-5173/

lipophilic systems (Liu et al., 2009; Saffari et al., 2016) have also been reported to significantly enhance skin permeation of various drugs.

Transdermal delivery of sparingly soluble drugs, especially those that are insoluble in water and other conventional solvents, is a great challenge. In recent years, ionic liquids (ILs), which have a set of ions and exist as a liquid at room temperature or below 100 °C (Roger and Seddon, 2003), have been widely used to increase the solubility of such drugs (Chowdhury et al., 2019a; Huang et al., 2019; Moniruzzaman et al., 2010a, 2010b). The drug permeation enhancing capacity of ILs is another important factor that must be taken into consideration (Sidat et al., 2019; Wang et al., 2018).

Although application of ILs in the pharmaceutical industry is significantly increasing, the two important parameters of ILs, cytotoxicity and degradability, are still now in under debate (Constable et al., 2007). Even though in the past few years, the uses of ILs in the pharmaceutical applications have been increased, most of them have not been exposed as ecologically and geologically friendly. It has been reported that the commonly used imidazolium, quinolinium, pyridinium, and fluorinates-based ILs exhibited as non-biodegradable and toxic to the environment and ecology (Adawiyah et al., 2016; Gomes et al., 2019; Sivapragasam et al., 2019). It has also been reported that imidazolium-based ILs showed higher toxicity toward cultured human keratinocytes cell line (HaCat) (Santos de Almeida et al., 2017). It is well confirmed that imidazolium-based ILs are not suitable because of their high toxicity and low biodegradability (Adawiyah et al., 2016; Amde et al., 2015). Interestingly, ILs containing organic (e.g., acetate, phosphate, carboxylate, amino acid), linear long chain (e.g., hexanoate, octanoate, and oleate) anions, and amino acid ester, choline, piperidinium, and pyrrolidinium cations are considered as readily biodegradable and non-toxic (Ali et al., 2019; Amde et al., 2015; De Santis et al., 2015; Hou et al., 2013). These important properties of ILs have opened a new avenue for selecting suitable biocompatible ILs for pharmaceutical purposes. It is interesting to note that because of the tunable properties, non-toxic ILs can be synthesized using biocompatible, biodegradable, and pharmaceutically acceptable organic cations and anions. The ILs composed of choline and amino acid (AA) are considered as the most safest and biocompatible IL (Chowdhury et al., 2019b; Nurunnabi et al., 2019). Choline is known as source of micronutrients and performs a vital role in the development of brain and memory development, and AAs are the most generous classes of organic molecules in universe, are generally regarded as safe (GRAS) and biocompatible (De Santis et al., 2015; Hou et al., 2013; Zeisel and Da Costa, 2009).

In this study, we developed potent biocompatible IL-based ternary systems containing isopropyl myristate (IPM), a pharmaceutically approved solvent, and ethanol (EtOH), a pharmaceutically approved co-solvent. Three ILs with choline as the cation and glycine, alanine, and serine as the anion, which were referred to as [Ch][Gly], [Ch][Ala], and [Ch][Ser], respectively, were used to investigate the solubility of a sparingly soluble drug (acyclovir, ACV). These ILs were biocompatible and nontoxic because of the biological sources of their cation and anions (Hou et al., 2013; Yazdani et al., 2016). Because the ILs were not able to transfer ACV into skin because of their strong hydrophilic nature, IPM and EtOH were incorporated in the ternary system. Here, IPM acted as a skin penetration enhancer (Eichner et al., 2017; Panchagnula et al., 2005; Zidan et al., 2017) and EtOH acted as a common solvent to overcome the problem associated with the miscibility between IL and IPM. Skin permeation of ACV using the IL-based ternary (IL–EtOH–IPM) systems and its effect on the skin barrier function were investigated using Yucatan micropig (YMP) full thickness skin. In addition, the *in vitro* cytotoxicity and skin irritation (biocompatibility) of the ILs and IL–EtOH–IPM systems were evaluated using mammalian fibroblast cells (L-929) and a reconstructed human epidermal model (LabCyte EPI-MODEL-12), respectively. Finally, in vivo histological analysis was performed to confirm the safety of the proposed ternary systems.

2. Materials and methods

2.1. Materials

ACV, IPM (purity ≥ 98.0%), and EtOH (purity > 99.9%) were purchased from Tokyo Chemical Industry Co., Ltd. (Tokyo, Japan). Choline chloride ([Ch][Cl]), silver oxide (Ag_2O), glycine, and L-serine were purchased from Sigma-Aldrich (Tokyo, Japan) and L-alanine was purchased from Wako Pure Chemicals Ltd. (Osaka, Japan). Opti-MEM, fetal bovine serum, Gibco minimum essential medium (MEM), and antibiotic–antimycotic solution were also purchased from Wako Pure Chemicals Ltd. Dulbecco's phosphate-buffered saline (D-PBS) and ethylene diamine tetraacetic acid/trypsin (1 mM ethylenediaminetetraacetic acid and 0.25% trypsin) solution were obtained from Nacalai Tesque (Kyoto, Japan). 2-(2-methoxy-4-nitrophenyl)-3-(4-nitrophenyl)-5-(2,4-disulfophenyl)-2H-tetrazolium (WST-8) and 3-[4,5-dimethylthiazol-2-yl]-2,5-di-phenyl-tetrazolium bromide (MTT) were provided by Dojindo Molecular Technologies, Inc. (Kumamoto, Japan). Milli-Q water was used in all of the experiments. All of the other reagents were analytical grade.

Female balb/c mice were obtained from CLEA Japan, Inc. Mice were accommodated under natural conditions (25 ± 2 °C, 60 ± 10% relative humidity) for one week prior to the experiments. Animals were nurtured and controlled as per guide line of 'Animal Ethics Committee' of Kyushu University, Japan. Mammalian fibroblast cell line L-929 was supplied by the RIKEN cell bank (Tsukuba, Japan). Reconstructed human epidermal model (LabCyte EPI-MODEL-12) was supplied by Japan Tissue Engineering Co., Ltd. (Gamagori, Japan).

2.2. Selection and synthesis of the ILs

All of the ILs containing choline as the cation and an AA as the anion were synthesized following a well-established method in our laboratory (Chowdhury et al., 2018). In brief, the choline AA ([Ch][AA]) ILs were synthesized by the two-step metathesis method (Fig. S1). In the first step, 5.0 g of [Ch][Cl] was mixed with Milli-Q water and stirred. An excess amount of Ag_2O was then added to [Ch][Cl] with vigorous stirring at room temperature and the solution was allowed to stand in the dark. After 2 h, the excess Ag_2O was removed by centrifugation (3500 rpm, 30 min) followed by filtration to obtain [Ch][OH] (choline hydroxide) aqueous solution. In the second step, the [Ch][OH] filtrate was neutralized with an aqueous solution of the AA by continuous stirring and allowed to stand for 24 h at room temperature. The solvent was removed by rotary evaporation (EYELA, NVC-2200, New York, USA) at 40 °C. An acetonitrile/methanol (9:1 v/v) mixture was then added to precipitate the unreacted AA, which was filtered off. The filtrate solution was evaporated again to remove the solvent and then freeze-dried for 48 h to completely evaporate the remaining solvent. Finally, successful synthesis of the ILs was confirmed by ^{1}H NMR, elemental analysis, and the Karl Fischer water content.

2.3. Solubility of ACV in the ILs and IL–EtOH and IL–H_2O mixtures

The optimum solubility of ACV in the ILs and IL–EtOH and IL–H_2O mixtures was determined using different weight ratios of the ILs and EtOH or H_2O (Table 1 and Fig. 1). In brief, an excess amount of ACV was added to each IL, IL–EtOH, and IL–H_2O system and they were then stirred at 25 °C for 24 h. The undissolved amounts of ACV were separated by filtration using a syringe driven filter (Millipore, 0.45 μm diameter). The ACV content in the filtrated solution was determined using an ultraviolet (UV) spectrophotometer at 252 nm with suitable dilution with methanol (MeOH) according to our previous report (Moniruzzaman et al., 2010b).

Table 1
Solubility of ACV in the [Ch][AA] ILs[a] at 25 °C and the effects of the viscosity, density, and anionic domain on IL-mediated dissolution[b].

IL or solvent	Anionic structure	Solubility of ACV (mg/mL)	ρ (g/cm^3)	η (Pa s)
[Ch][Gly]	R = −H	250 ± 17$^{****, **}$	1.16 ± 0.03	1.23 ± 0.11
[Ch][Ala]	R = −CH3	210 ± 15****	1.14 ± 0.03	0.82 ± 0.08
[Ch][Ser]	R = HO	135 ± 11****	1.20 ± 0.03	11.73 ± 0.83
EtOH	–	0.11 ± 0.01	0.79[c]	1.20[c]
IPM	–	0.03 ± 0.005	0.85[c]	5.75[c]
EtOH-IPM(1:1 wt ratio)	–	0.05 ± 0.01	–	–
H_2O	–	0.43 ± 0.10	–	–

[a] The solubility of ACV in EtOH, water and IPM are also given.
[b] Data are shown as mean ± SD (n = 3).
[c] Values were taken from catalogue.
**** Compared with H_2O, EtOH, IPM, and EtOH–IPM solutions, $p < 0.0001$.
** Compared with [Ch][Ala] and [Ch][Ser], $p < 0.01$ using Sidak's multiple comparison test.

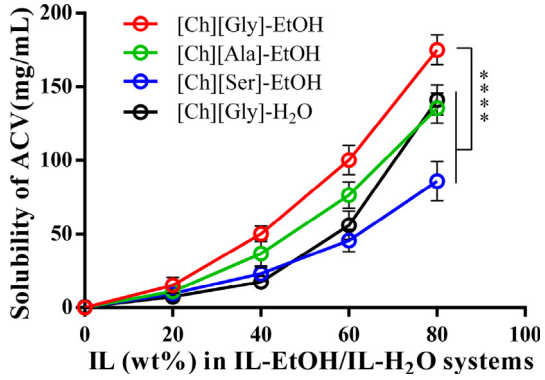

Fig. 1. Solubility of ACV in various IL–EtOH and IL–H_2O systems at 25 °C (mean ± SD, $n = 3$, ****$p < 0.0001$ using Dunnett's multiple comparison test).

2.4. Phase behavior of the IL–EtOH–IPM ternary systems

The phase behavior of the IL–EtOH–IPM systems was investigated at different weight ratios. First, the IL was mixed with EtOH at different weight ratios followed by continuous addition of IPM to that mixture until it turned turbid. In the IL–EtOH–IPM systems, the concentration of the IL was varied from 1 to 50 wt%. The temperature of the experiments was maintained at 25 ± 2 °C.

2.5. Preparation of the IL–EtOH–IPM ternary systems

To prepare the IL–EtOH–IPM ternary systems, the ILs (2, 4, 10 and 15 wt%) were mixed with EtOH (25, 35, 50, and 60 wt%, respectively) followed by thorough vortexing at 25 °C. The required amount of IPM was then added to each solution and the solution was vigorously vortexed until a clear and optically transparent solution was obtained. For preparation of the H_2O–EtOH–IPM ternary system, water was added instead of the IL. For the transdermal drug delivery experiments, the IL–EtOH–IPM systems were prepared by adding an appropriate amount of IPM to IL–EtOH in which a fixed amount of the drug (ACV) was solubilized in advance.

2.6. Drug solubility determination in the IL–EtOH–IPM ternary system

The solubility of AVC in the IL–EtOH–IPM ternary systems was determined as described in the Section 2.3. In brief, a saturated amount of ACV was added to each IL/EtOH mixture (2/25, 4/35, 10/50, and 15/60 wt%) by stirring at 25 °C for 24 h. An appropriate amount of IPM (73, 61, 40, and 25 wt%, respectively) was then added with vortexing. The undissolved amounts of ACV were separated by filtration using a syringe driven filter (Millipore, 0.45 μm diameter). The ACV content in the filtrated solution was determined using an UV spectrophotometer at 252 nm with suitable dilution with MeOH.

2.7. Characterization of the ILs and IL–EtOH–IPM ternary systems

The instruments used to determine the physical properties (viscosity and density) were calibrated using Millipore-quality water before taking the reading, as instructed by the supplier. An Anton Paar microviscometer (Lovis, 2000 M/ME, Graz, Austria) and an Anton Paar density meter (DMA 35 N) were used to measure the viscosity and density of the ILs and IL–EtOH–IPM systems at a temperature of 25 ± 0.01 °C. To measure the viscosity, the samples were added to a glass capillary containing a rolling steel ball. The viscosity of the tested sample was determined by measuring the rolling time of the steel ball.

2.8. Skin permeation study

In vitro drug release was investigated using full thickness YMP skin. Franz diffusion cells with 10 mm diameter were used to perform the drug release into the skin (topical) and across the skin (transdermal) experiments according to the previous reports (Piao et al., 2008; Tahara et al., 2008). In brief, the YMP skin was first cut into the desired size. The skin was then clamped between the donor and receiver compartments of the Franz diffusion cell containing D-PBS solution (pH 7.4) in the receiver compartment. The skin was clamped in such a way that the sc faced the donor side and the dermal part faced the receiver side and was in contact with the D-PBS solution. It should be noted that the YMP skin pieces were hydrated for 1 h with D-PBS before setting them in the diffusion cell. For the skin permeation study, 0.5 mL of the test formulation was placed in the donor compartment and 5 mL D-PBS solution was placed in the receiver compartment. The receiver compartment was magnetically stirred at 550 rpm and the temperature was kept constant at 32.5 °C during the entire experiment using a circulating water bath (NTT-20S, Tokyo Rikakikai Co. Ltd., Tokyo, Japan). To determine the drug content in the receiver phase (transdermal delivery) after a fixed time interval, 0.5 mL of the receiver solution was replaced with the same amount of fresh D-PBS solution. After a predetermined time, the donor solution was removed from the skin. The skin was then unclamped and washed twice with 0.1 M HCl acid to remove the drug from the outer surface of the skin. Finally, the treated skin was processed according to our previous report (Tahara et al., 2008) to estimate the topical drug delivery content. ACV was determined by HPLC using a Shiseido Capcell Pak C18 MG column (4.6 mm × 250 mm) using the

United States Pharmacopeia (USP) method at 254 nm. Here, the mobile phase was 0.02 M glacial acetic acid with a flow rate 1.5 mL/min, the injected volume was 100 μL, the oven temperature was 40 °C, and the retention time was about 12 min. The squared correlation coefficient of the standard curve was greater than 0.99 ($R^2 > 0.99$) when the standard solutions were 0–25 μg/mL (Fig. S2).

2.9. Calculation of skin permeation parameters

To estimate the transdermal flux, the cumulative amount of the permeated drug through the unit surface area of the YMP skin was plotted against the permeation time. The transdermal flux (J, μg/cm^2/h) was the slope of the curve. The skin permeability coefficient (K_P, cm/h) was calculated with the equation $K_P = J/C_d$, where C_d (mg/mL) is the concentration of the drug in the donor phase. Lag time (t_L, h) was the intercepts of X-axis and the diffusion coefficient in the skin (D, cm^2/h) was derived from the lag time by the equation $D = l^2/6t_L$, where l (cm) is the thickness of the full YMP skin. Skin partition coefficient, (K_{skin}), was determined by the equation: $K_{skin} = (Jl)/(DC_d$.

2.10. Influence of the [Ch][Gly]-based ternary system on the skin permeability

The effect of the IL–EtOH–IPM ternary system on the skin barrier function was investigated by Fourier transform infrared (FTIR) spectroscopy (PerkinElmer, version 10.5.2, USA). The YMP skin was prepared by a previously reported method (Wang et al., 2018). In brief, the full thickness skin was frozen and then kept at room temperature for 1 h. The total fat portion was then cut off. After moisture removal, the skin was incubated at 60 °C for 1–2 min to loosen the epidermis. The epidermis of the skin was then gently removed using forceps and floated on 0.25% trypsin and 1 mM ethylenediaminetetraacetic acid solution keeping the sc side facing up for 24 h at room temperature. After isolation, the sc was washed with water and dried at room temperature for 24 h. The sc was cut into the desired size and the FTIR spectrum was recorded as the control. The sc was then soaked in the test sample for 30 min. Finally, the treated sc was thoroughly washed with 20% EtOH, allowed to dry for 1 h, and analyzed by FTIR spectroscopy. Finally, the FTIR spectrum of the treated sc was compared with the control spectrum.

2.11. In vitro cytotoxicity study

The WST-8 cell viability assay was performed using mammalian fibroblast cell line L-929 according to a previous reported method with some modifications (Moshikur et al., 2018). The fibroblast cells were cultivated in a cell culture dish at 37 °C for 24 h in a CO_2 incubator. After cultivation, the cells were collected from the dish by trypsinizing. The target cells were seeded in a 96-well flat-bottomed plate at 5000 cells/well with 100 μL MEM containing 10% fetal bovine serum and 1% antibiotic–antimycotic solution and then incubated again for 24 h at the same conditions as above. Different concentration solutions (20–300 mM) of the [Ch][AA] ILs, the conventional ILs 1-butyl-3-methylimidazolium imidazolium chloride ([Bmim][Cl]) and dimethylimidazolium dimethylphosphate ([C1mim][DMP]), and [Ch][Cl] were prepared with Opti-MEM. The MEM from each well was replaced by 100 μL of the prepared solution and incubated for 24 h. After incubation, the test solution from each well was removed and washed twice with D-PBS to completely remove the test solution. To investigate the mitochondrial activity of the cells, 100 μL of Opti-MEM containing 10% (w/w) WST solution was added to each well and then allowed to stand for incubation. After 3 h incubation, the absorbance of the supernatant ($A_{treated}$) at 450 nm was measured with a microplate spectrophotometer (iMARK, Bio-Rad, Tokyo, Japan). The absorbance of the cells soaked in Opti-MEM ($A_{control}$) was used as the control. The relative cell viability was calculated with the following equation:

$$\text{Cell viability}(\%) = (A_{treated}/A_{control}) \times 100$$

Finally, the half maximal inhibitory concentration (IC_{50}) values of the tested samples were calculated.

2.12. In vitro skin irritation study

An *in vitro* skin irritation study was performed using the reconstructed human epidermal model LabCyte EPI-MODEL-12 according a previously reported method with some modifications (Moniruzzaman et al., 2010b). In brief, the tissues were cultured into 24-well plates (BD Biosciences, San Jose, CA, USA) with Dulbecco's assay medium (0.5 mL) and incubated at 37 °C in 5% CO_2 overnight. Subsequently, 25 μL of the test sample (F1, F7, [Ch][Gly], and IPM) was added to each well and incubated at 37 °C in 5% CO_2 for 6 h. D-PBS and [C1mim][DMP] were used as the negative and positive control, respectively. The tissues were then carefully rinsed 15 times with D-PBS to completely remove the test samples from the tissue surface. Thereafter, 0.5 mL of the assay medium containing 0.5 mg/mL MTT was added to each well followed by incubation for 3 h under the same conditions. The tissues were then shifted to microtubes containing 300 μL 2-propanol and complete immersion was confirmed. The microtubes were covered with aluminum foil and refrigerated for 2 days. Samples of the solutions (100 μL) were extracted and transferred to 96-well plates, and the optical density was measured at 570 and 650 nm using a microplate reader (iMARK, Bio-Rad, Tokyo, Japan). The cell viability percentage was calculated by comparing with the viability of D-PBS as the negative control and propanol-2 as the blank.

2.13. In vivo histological study

Histological analysis was performed to determine the skin irritation of the IL-based ternary systems using female balb/c mice according to the previous reports (Wang et al., 2018; Wu et al., 2019). In brief, twelve mice were distributed in four groups (4 × 3). The dorsal hairs of the mice were removed. Then 150 μL of IL–EtOH–IPM (F1), IL–EtOH–H_2O (15:35:50 wt%), and [Bmim][Cl]–EtOH–H_2O (15:35:50 wt%) were applied on dorsal areas using a home-made patch (approximately 1.5 cm × 1.5 cm) for 24 h whereas same volumes of D-PDS were applied as control. Then the mice were sacrificed and treated dorsal areas were removed, washed with Milli-Q and followed by immersing in Histo Prep compound (Fisher Scientific, NJ, USA) and maintaining at − 80 °C. The skin samples were then segmented with a cryostat microtome (Leica CM1860 UV, Wetzlar, Germany) and fixed on glass slides. The glass slides were subsequently stained with hematoxylin and eosin (Muto Pure Chemicals Co., Ltd., Tokyo, Japan). Finally, the stained skin samples were observed through a 40 × objective lens with a fluorescence microscope (BZ-9000 BIOREVO, Keyence Corp., USA).

2.14. Statistical data analysis

The data are given as the mean ± standard deviation (SD). The comparisons between more than two groups were performed by two-way ANOVA analysis for multiple comparison tests using GraphPad Prism software (Version 6.05). The differences were considered significant at $p < 0.05$.

3. Results and discussion

3.1. Selection of ILs based on the biocompatibility

In this study, a group of biocompatible ILs consisting of the choline as the cation and an AA (glycine, alanine or serine) as the anion ([Ch][AA] IL) were selected to investigate the solubility of the practically water insoluble drug ACV, followed by development of a new potential IL-based TDDS. Synthesis of the ILs was successfully completed and confirmed by ^{1}H NMR, elemental analysis, and the Karl Fischer water

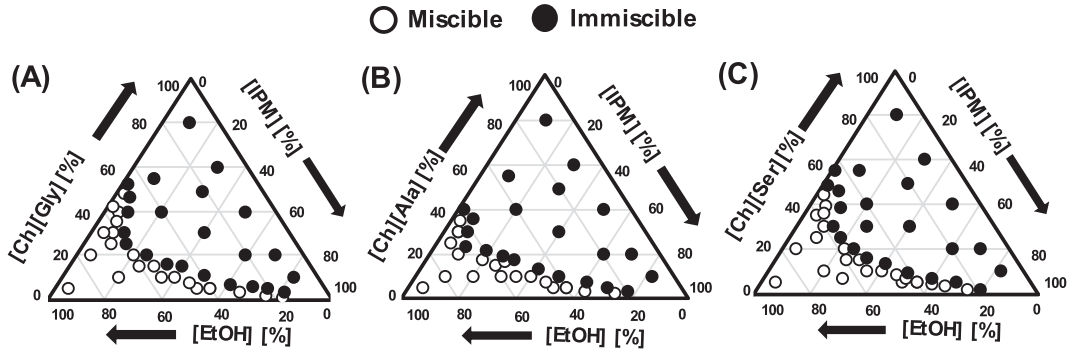

Fig. 2. Pseudo ternary phase diagrams of the (A) [Ch][Gly]–EtOH–IPM, (B) [Ch][Ala]–EtOH–IPM and (C) [Ch][Ser]–EtOH–IPM systems at 25 °C.

content, and the results were in good agreement with previous study (Chowdhury et al., 2018). The most important issues for use of a chemical in a drug delivery system are the toxicity and biocompatibility. For the [Ch][AA] ILs, both of the cationic and anionic portions are considered to be safe and non-toxic because choline is a source of macronutrients and AAs are the building block of proteins with a wide range of nutritional values (Zeisel and Da Costa, 2009). [Ch][AA] ILs are completely composed of renewable biomaterials showing low toxicity toward bacteria and classified as readily biodegradable (De Santis et al., 2015; Hou et al., 2013). Therefore, the [Ch][AA] ILs were considered to be green solvents for the drug delivery systems developed in this study.

3.2. Solubility of ACV in the [Ch][AA] ILs and the relation with the physical properties

Two fundamental properties of the [Ch][AA], the viscosity and density, were measured (Table 1). The viscosity (η) of the [Ch][AA] was significantly different, ranging from 0.82 Pa s for [Ch][Ala] to 11.73 Pa s for [Ch][Ser]. It has been reported that the viscosities of [Ch][AA] were significantly higher than those of most common ILs, and the measured viscosities were in reasonable agreement with the literature (De Santis et al., 2015). The viscosity of a solvent is directly related to the structure, symmetry, and molecular weight of the cations and anions (Muhammad et al., 2011). The measured densities (ρ) of the [Ch][AA] significantly varied from 1.14 to 1.20 g/cm^3. However, the relations of the viscosity and density with the structure, molecular weight, and side chain of the IL anion could not be established in this study.

ACV is sparingly soluble in water and most organic solvents but highly soluble in [Ch][AA]. The solubility of ACV in the [Ch][AA] and other solvents was determined by constructing a calibration curve with different ACV concentration solutions (2–10 μg/mL) and obtaining the maximum wavelength of ACV (**Fig. S3**). The ACV solubility in the ILs was significantly higher than in water and commonly used organic solvents (< 0.43 mg/mL in water, < 0.11 mg/mL in EtOH, < 0.03 mg/mL in IPM, and < 0.05 mg/mL in EtOH–IPM). For the [Ch][AA], the maximum ACV solubility was ~ 250 mg/mL in [Ch][Gly], and minimum ACV solubility was ~ 135 mg/mL in [Ch][Ser] (Table 1). The solubility of ACV was highly dependent on the density, viscosity, and nature of the anion. It has been reported that the solubilizing ability of ILs is strongly related to the density (Abe et al., 2015) and viscosity (Fukaya et al., 2006) of the IL. ILs are considered to assist solubilization of drug molecules through the anions, which directly bind to the drug by hydrogen bonding, van der Waals forces, or π–π interactions (Moniruzzaman et al., 2010a). Glycine, which is the smallest and simplest AA, has higher surface electron density than other AAs, and it easily and strongly participates in [Ch][Gly]–ACV complex formation to govern the ACV dissolution, and hence ACV shows the highest solubility in [Ch][Gly] (Chowdhury et al., 2018).

3.3. Solubility of ACV in the IL–EtOH and IL–H_2O systems

The solubility of ACV in the IL–EtOH and IL–H_2O systems was investigated using IL–EtOH and IL–H_2O systems with different compositions (Fig. 1). The solubility of ACV in EtOH and H_2O was very low. Interestingly, the presence of IL in the IL–EtOH and IL–H_2O systems significantly enhanced the solubilization efficiency, and the ACV solubility increased with increasing IL content. The solubility of ACV was significantly higher in the IL–EtOH system than in the IL–H_2O system (e.g., [Ch][Gly]–EtOH and [Ch][Gly]–H_2O), even though ACV had lower solubility in EtOH than in H_2O. In addition, the solubility of ACV in the [Ch][Gly]–EtOH system was significantly higher than in the other IL–EtOH systems. The ACV solubility was in the following order: [Ch][Gly]–EtOH > [Ch][Ala]–EtOH > [Ch][Ser]–EtOH.

3.4. Phase behavior study of the IL–EtOH–IPM ternary systems

In this study, we focused on transdermal delivery of ACV. It has been reported that IL–ACV mixtures are not suitable for topical and transdermal delivery owing to the hydrophobic barrier of the skin (Moniruzzaman et al., 2010b; Szumała et al., 2019). To overcome the barrier function, in this study, we used IPM as a hydrophobic oil. EtOH was used as a co-solvent to solve the immiscibility of IL and IPM. Furthermore, the use of ethanol as a co-solvent in pharmaceutical formulation have been widely accepted to enhance the drug solubility and permeability across the biological membrane (Pramanick et al., 2013; Strickley, 2004). The phase diagrams of the ILs, EtOH, and IPM were used to develop the pseudo ternary phase diagrams of the IL–EtOH–IPM systems, where EtOH is miscible with both the hydrophilic [Ch][AA] ILs and hydrophobic IPM at any proportion (Fig. 2). From the phase behavior study, all three of the [Ch][AA] had excellent IL–EtOH–IPM system formation capacity, which is indicated by the miscible area in the ternary diagram, and there was no significance difference in the miscible areas of the three ILs. To use a high IL content in the system, a high content of EtOH and a low content of IPM must also be used, which were not suitable for the proposed delivery system. Similarly, a high IPM content cannot be used owing to the conflict with the low IL content. For a TDDS, it is beneficial to use as high IL and IPM contents as possible with a low EtOH content. Therefore, the optimized compositions of the ternary systems were investigated.

3.5. Drug loading in the IL–EtOH–IPM systems

The ACV loading capacities of the IL–EtOH–IPM ternary systems were determined to assess their abilities as TDDSs for the sparingly soluble drug ACV. The ACV loading capacities for different contents of IL, EtOH, and IPM were determined. The ACV loading capacity significantly varied owing to the high dependency of the drug solubility on the individual contents of the systems. The ACV loading capacity was significantly lower in the EtOH–IPM system (~0.05 mg/mL, Table 1)

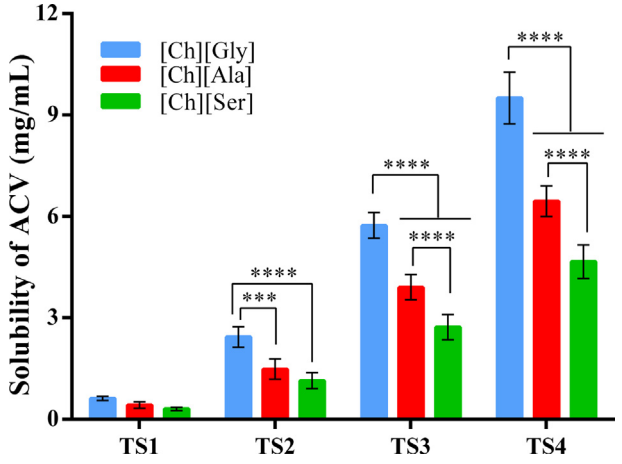

Fig. 3. Drug loading in various IL–EtOH–IPM formulations at 25 °C (mean ± SD, $n = 3$, ***$p < 0.001$ and ****$p < 0.0001$ using Sidak's multiple comparison test). TS1: 2 wt% IL, 25 wt% EtOH, and 73 wt% IPM. TS2: 4 wt% IL, 35 wt% EtOH, and 61 wt% IPM. TS3: 10 wt% IL, 50 wt% EtOH, and 40 wt% IPM. TS4: 15 wt% IL, 60 wt% EtOH and 25 wt% IPM.

than in the [Ch][AA] systems. Upon addition of IL to the system, the ACV loading capacity remarkably increased (Fig. 3). The ACV loading capacity and IL content in the ternary system were proportionally related. Interestingly, the [Ch][Gly] based ternary system showed higher ACV loading capacity than the [Ch][Ala] and [Ch][Ser] based ternary systems. At any weight ratios of IL, EtOH, and IPM, the ACV loading capacity was always higher for the [Ch][Gly]-containing system, and it was significantly higher when IL ≥ 4.0 wt% (Fig. 3). This could be because of the anion effect on dissolution. It is well known that IL-mediated dissolution of hydrophobic entities (e.g., drugs and cellulose) is mainly governed by the anions. Small anions have higher electronegativity and higher dissolution ability than large anions (Chowdhury et al., 2018).

3.6. Selection of the IL–EtOH–IPM system for the skin permeation study

The components and compositions for preparation of pharmaceutically acceptable formulations should be non-toxic and stable. IPM and the IL were considered to play the most important roles in skin permeation and drug loading, respectively. A system containing higher IL content can incorporate more drug. However, higher IL content required higher EtOH content, resulting in lower IPM content (less permeation). For preparation of effective IL–EtOH–IPM ternary systems for transdermal delivery, the optimum IL, EtOH, and IPM contents were chosen (Table 2). Ternary systems 1–4 (F1–F4) contained [Ch][Gly], and F5, F6 and F7 contained [Ch][Ala], [Ch][Ser] and H_2O,

Table 2
Compositions of the different systems for the skin permeation study[a].

Formulations	Compositions				ρ (g/cm^3)	η (mPa s)
	IL or H_2O (wt.%)		EtOH (wt.%)	IPM (wt. %)		
F1	[Ch][Gly]	4	35	61	0.833 ± 0.008	3.16 ± 0.06
F2		4	45	51	0.824 ± 0.005	3.11 ± 0.01
F3		10	50	40	0.844 ± 0.002	3.71 ± 0.02
F4		15	60	25	0.859 ± 0.005	3.92 ± 0.08
F5	[Ch][Ala]	10	50	40	0.842 ± 0.002	3.28 ± 0.07
F6	[Ch][Ser]	10	50	40	0.847 ± 0.008	3.84 ± 0.09
F7[b]	H_2O	4	35	61	–	–

[a] The density and viscosity data are given as the mean ± SD ($n = 3$).
[b] F7 was set as the control.

Table 3
ACV penetration into and across the skin using [Ch][Gly] IL-based formulations at 32.5 °C (mean ± SD, $n = 3$)[a].

Formulations	Transdermal delivery (μg/cm^2)	Topical delivery (μg/cm^2)
IL	ND	ND
IL-H_2O (1:1 wt%)	ND	ND
EtOH[b]	ND	0.08 ± 0.03
IPM[b]	ND	0.17 ± 0.06
IL-EtOH (1:1 wt%)	1.91 ± 0.13	4.12 ± 0.20
IL-EtOH-IPM[c]	58.26 ± 2.01****	33.33 ± 2.15****
H_2O-EtOH-IPM[b,d]	ND	0.22 ± 0.05

[a] All of the systems contained 2 mg/mL ACV and the penetration time was 24 h.
[b] Almost all of the ACV remained as a suspended powder in the system.
[c] IL–EtOH–IPM (ME1) (Table 2) containing 4 wt% [Ch][Gly].
[d] H_2O–EtOH–IPM (ME7) (Table 2) containing 4 wt% H_2O instead of IL.
**** Compared with other systems, $p < 0.0001$ using Dunnett's multiple comparison test.

respectively. The densities and viscosities of the systems were measured in the absence of ACV as a control. In the [Ch][Gly] containing systems, the density and viscosity increased with increasing IL content (F4 > F3 > F1). Among the systems containing 10 wt% IL, F6 had the highest viscosity value owing to the high viscosity of [Ch][Ser] (Abe et al., 2015; Fukaya et al., 2006) and the viscosity was in the order Ser > Gly > Ala.

3.7. Skin permeation study

In vitro permeation of the ACV-loaded formulations (2 mg/mL) was investigated using YMP full thickness skin. The YMP skin was selected as a model skin because its clinical, structural, reactivity, and immunohistochemical features remarkably resemble those of human skin (Summerfield et al., 2015). First, the transdermal (across the skin) and topical (into the skin) delivery of ACV were measured for the [Ch][Gly], EtOH, IPM, [Ch][Gly]–H_2O, [Ch][Gly]–EtOH, [Ch][Gly]–EtOH–IPM, and H_2O–EtOH–IPM systems (Table 3). It should be noted that ACV was solubilized in the IL, IL–EtOH, IL–H_2O, and IL–EtOH–IPM systems but it remained as a suspension (not solubilized) in the other systems. The IL–EtOH–IPM system significantly enhanced transdermal permeation of ACV, whereas the other systems, except for IL–EtOH, showed no transdermal permeation (below the detection limit). For the IL–EtOH–IPM system, the transdermal and topical permeation were 58.26 and 33.33 μg/cm^2, respectively, whereas for IL–EtOH, the corresponding values were 1.91 and 4.12 μg/cm^2, respectively. There were two main factors for excellent permeation of the IL–EtOH–IPM systems. First, the high concentration gradient provided by the large amount of fully soluble drug in the system (Moniruzzaman et al., 2010b; Sintov and Shapiro, 2004). Second, the disruption ability of IPM to overcome the barrier function of the sc lipid structure (Panchagnula et al., 2005; Wang et al., 2018). For the ACV-loaded IL, the drug was fully solubilized but did not diffuse into the skin owing to the highly hydrophobic barrier function of the sc, and the strong hydrophilic nature of the ILs (Karande and Mitragotri, 2009; Moniruzzaman et al., 2010b; Szumała et al., 2019). Though IPM and IL–EtOH–IPM systems can overcome the barrier function, ACV could not permeate across the skin because ACV was suspended in these systems, which probably obstructed the skin (Moniruzzaman et al., 2010b).

A group of IL–EtOH–IPM ternary systems containing different ILs and with different compositions was then used to evaluate the transdermal and topical permeation of ACV. The transdermal profile showed that the cumulative drug amount at 24 h (Q_{24}) for F1 was significantly higher than other ternary systems as shown in Fig. 4. Other permeation parameters, including J, t_L, K_P, D, and K_{skin} were also determined from the transdermal profile and presented in Table 4. All the permeation

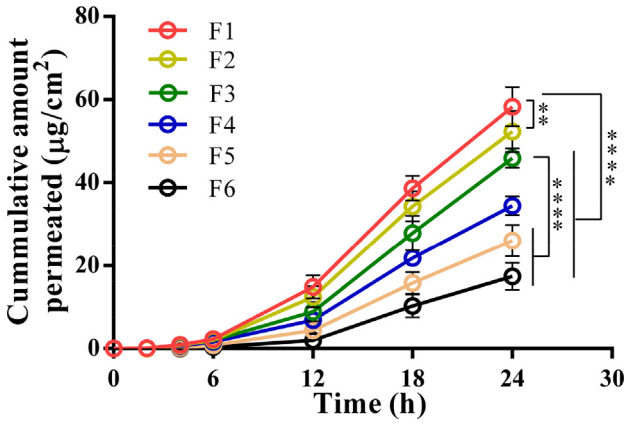

Fig. 4. Permeation profiles of ACV across the skin for different IL–EtOH–IPM ternary systems at 25 °C (mean ± SD, $n = 3$, $^{**}p < 0.01$ and $^{****}p < 0.0001$ using Sidak's multiple comparison test).

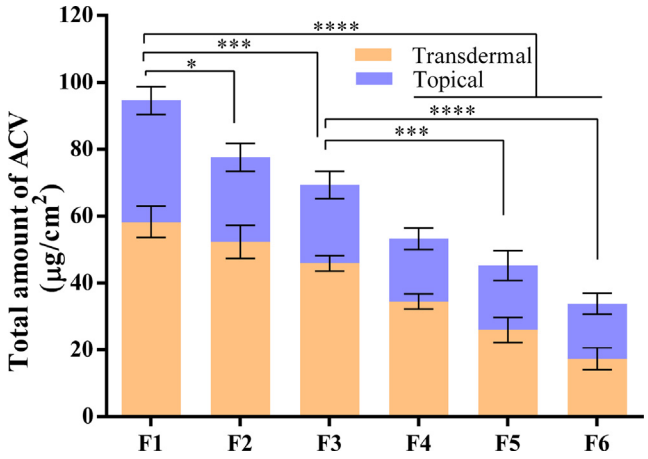

Fig. 5. The sum of transdermal and topical delivery of ACV after 24 h (mean ± SD, $n = 3$, $^{*}p < 0.05$, $^{***}p < 0.001$, and $^{****}p < 0.0001$ using Sidak's multiple comparison test).

parameters, especially J and K_P, of F1 were significantly higher than other ternary systems. The total (transdermal and topical) delivery amount of ACV at 24 h were determined and it was found that the total delivery amount of ACV was significantly higher for F1 compared with other ternary systems (Fig. 5).

Generally, the transdermal permeation of drug is proportionally related to J and K_p. The presence of high amount of IPM was mainly responsible for high K_{skin} of F1. Furthermore, D was maintained at higher level due to the balanced composition of EtOH and IPM for F1, resulting a balanced "push" and "pull" effect of high J and K_p (Panchagnula et al., 2005).

As F1 showed the significantly higher J and K_p than other ternary systems, which are favourable for the transdermal delivery, could be the best candidate for the delivery of ACV (Table 4).

3.8. Effect of the [Ch][Gly]-based ternary system on the ACV skin permeability

FTIR spectroscopy, which can provide deep insight into the molecular structure of the lipid matrix of the sc (Kumar et al., 2015; Schwarz et al., 2013), was performed to evaluate the structural changes of the sc (Shah et al., 2008). The control systems of F1, F7, and IPM were used because ACV itself is unlikely to interfere with the skin structure. For control sample (untreated), the characteristic absorption peaks of the lipid were located at 2920 (C−H asymmetric vibration), 2851 (C–H symmetric vibration), and 1731.5 cm^{-1} (C═O vibration), and the peaks of keratin were located at 1643.5 and 1538.25 cm^{-1} (NH−C═O vibration). All the treated skin produced some peaks shifts for both the lipid and keratin of the sc (Fig. 6 and Table 5). Moreover, F1 had a more significant effect on structural change of the skin compared with F7 and IPM alone because of the synergistic enhancing effect of the multiple components in the system (Kim et al., 2008; Liu et al., 2009; Panchagnula et al., 2005). For the F1 system, the C−H vibration peaks shifted to 2924.25 (asymmetric vibration) and 2854.75 cm^{-1} (symmetric vibration), the C═O peaks shifted to 1734 cm^{-1}, and the NH−C═O peaks shifted to 1647.5 and 1542.75 cm^{-1}. These changes in the vibration peaks were directly connected to molecular organization of the sc (Schwarz et al., 2013). For the F1 system, the CH_2 symmetric stretching vibration peak shifted to higher wavenumber because of transformation of the lipid from an orthorhombic conformation to a liquid-crystalline structure, which indicated a more fluid structure. Moreover, the NH–C═O vibration peaks shifting to higher wavenumber revealed that the conformation of keratin converted from an organized α-helical structure to a randomly coiled structure by treatment with the test systems. The aforementioned results confirmed the influence of the F1 system on the skin barrier properties, which can be ascribed to the ionic character of the IL(Wang et al., 2018; Zheng et al., 2020). Additionally, the effect of EtOH–IPM in the F1 system can be attributed to the optimum balance of push–pull and blending effects in the skin. This balance of the push–pull and blending effects decreases the barrier function of skin, leading to a higher permeability coefficient and better transdermal delivery (Wang et al., 2018).

3.9. In vitro cytotoxicity study

The biocompatibility of ILs were investigated by evaluating their cytotoxicity using fibroblast cells (L-929). The calculated IC_{50} values of ILs used in this study were compared with those of two imidazolium-based IL, [C1mim] [DMP] and [Bmim][Cl], as positive control and [Ch][Cl], as a negative control. The IC_{50} values of all of [Ch][AA] were significantly higher than those of [Bmim][Cl] and [C1mim][DMP]), and similar to that of [Ch][Cl], indicating no or less toxicity of [Ch][AA] (Fig. 7). These results were in a good agreement with published

Table 4
ACV skin permeation parameters for ternary systems containing different [Ch][AA] ILs and with different compositions; (Mean ± SD, n = 3).

Formulations	J (μg/cm²/h)	t_L (h)	K_P ($\times 10^{-4}$ cm/h)	D ($\times 10^{-4}$ cm²/h)	K_{Skin}
F1	3.62 ± 0.34	7.55 ± 1.2	18.08 ± 3.5	6.68 ± 0.73	0.47 ± 0.12
F2	3.32 ± 0.31*	8.05 ± 1.2	16.61 ± 3.3*	6.27 ± 0.66	0.46 ± 0.11
F3	2.81 ± 0.23***	8.57 ± 1.3	14.03 ± 3.1**	5.89 ± 0.62	0.41 ± 0.09
F4	2.24 ± 0.21****	8.72 ± 1.4	11.22 ± 2.6***	5.79 ± 0.54	0.33 ± 0.08
F5	1.80 ± 0.19****	9.46 ± 1.4	9.01 ± 2.2****	5.33 ± 0.55	0.29 ± 0.07
F6	1.28 ± 0.18****	10.28 ± 1.5	6.40 ± 1.4****	4.91 ± 0.48	0.23 ± 0.07

* $p < 0.05$.
** $p < 0.01$.
*** $p < 0.001$ and.
**** $p < 0.0001$ compared with F1 using Dunnett's multiple comparisons test.

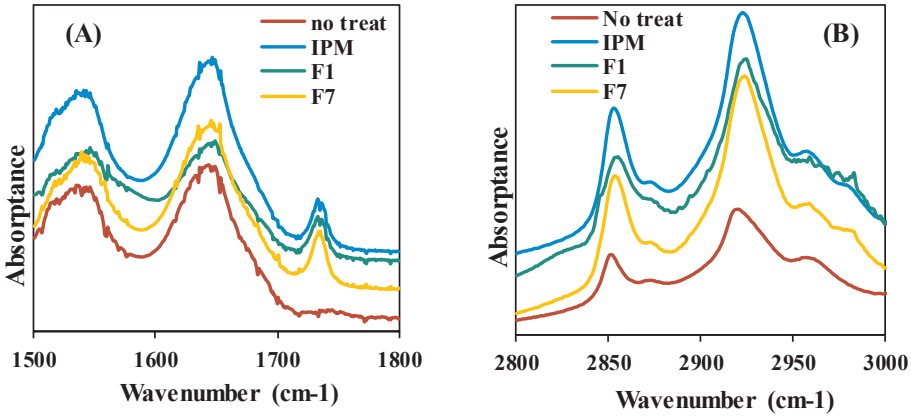

Fig. 6. FTIR spectra of sc samples after treatment with different formulations.

Table 5
FTIR peak shifts of the sc after treatment with different systems (mean ± SD, n = 3).

SC components		No treat	IPM		F1		F7	
		Absorption	Absorption	ΔShift	Absorption	ΔShift	Absorption	ΔShift
Lipid	CH_2, Asymm (cm^{-1})	2920.25 ± 0.05	2922.5 ± 0.08	2.25	2924.25 ± 0.1	4	2923.25 ± 0.1	3
	CH_2,Symm (cm^{-1})	2851.25 ± 0.06	2852.75 ± 0.1	1.50	2854.75 ± 0.2	3.50	2853.25 ± 0.1	2
	C = O (cm^{-1})	1731.5 ± 0.08	1733.5 ± 0.1	2	1734 ± 0.09	2.5	1734 ± 0.1	2.5
Keratin	NH-C = O (cm^{-1})	1643.5 ± 0.1	1646.5 ± 0.09	3	1647.5 ± 0.1	4	1646.5 ± 0.08	3
		1538.25 ± 0.11	1540.75 ± 0.1	2.5	1542.75 ± 0.1	4.5	1541.75 ± 0.9	3.5

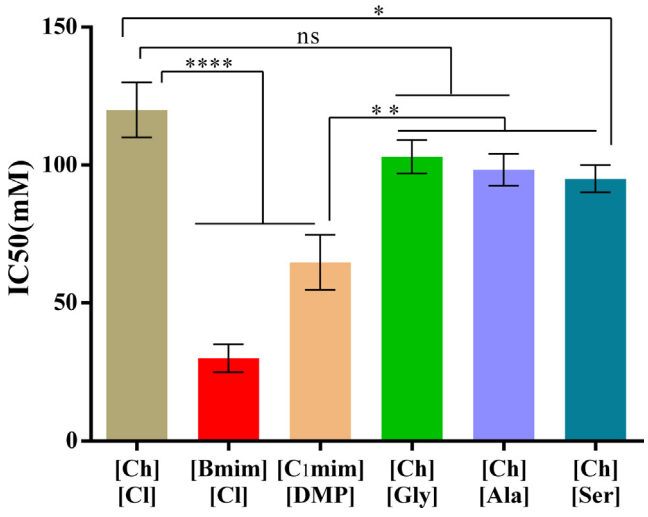

Fig. 7. In vitro cytotoxicity of [Ch][AA] and conventional ILs (mean ± SD, n = 3, ns: not significant, *p < 0.05, **p < 0.01 and ****p < 0.0001 using Sidak's multiple comparison test).

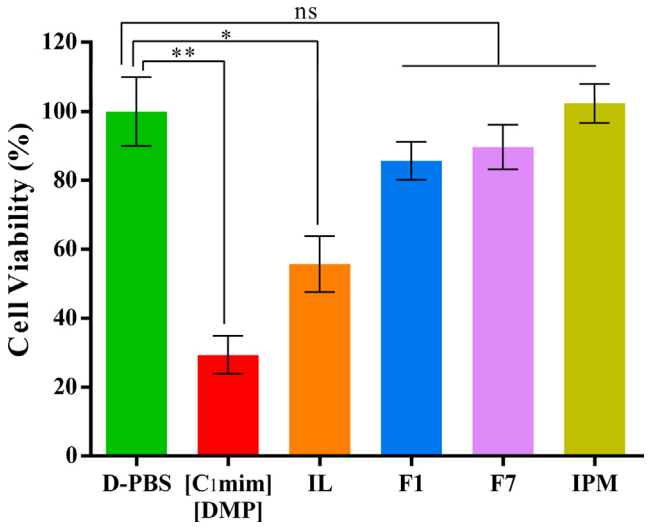

Fig. 8. Cytotoxicity evaluation of [Ch][Gly] and [Ch][Gly]-based ternary system using reconstructed human epidermal model LabCyte EPI-MODEL-12 (mean ± SD, n = 3), ns: not significant, *p < 0.05 and **p < 0.01 compared to D-PBS using Dunnett's multiple comparisons test.

reports where choline-based ILs exposed no or less toxicity on MCF-7, SK-MEL-28, and MRC-5 cell line (Gomes et al., 2019; Muhammad et al., 2011). It has been reported that choline-based ILs showed lower toxicity than imidazolium-based ILs on MCF-10 and Hela cell line (Gouveia et al., 2014; Lotfi et al., 2017). The cytotoxicity increased in the order [Ch][Gly] < [Ch][Ala] < [Ch][Ser] with no significant difference, which was in a good agreement with the literatures (Chowdhury et al., 2018; Hou et al., 2013; Yazdani et al., 2016). Although the anions play a vital role on toxicity, the ILs used in this study contained AA as anion, which are well known to be safe, non-toxic, and biodegradable (Gomes et al., 2019; Sivapragasam et al., 2019; Yazdani et al., 2016). Therefore, the [Ch][AA] were considered to be non-toxic and biocompatible.

3.10. In vitro skin irritation study

The *in vitro* skin irritation profiles of the [Ch][Gly] and its formulation, F1, were evaluated using a reconstructed human epidermal model (LabCyte EPI-MODEL), and compared with those of the commercially available IL, [C1mim] [DMP], which has already been reported to be an irritant under the same experimental setup (Moniruzzaman et al., 2010b). F1 showed high cell viability > 85% compared with the negative control, D-PBS and the value was not significantly differed from D-PBS, IPM and F7 (water-based ternary system) as shown in Fig. 8. The results indicated the ultimate biocompatibility of IL-based ternary system. However, when [Ch][Gly]

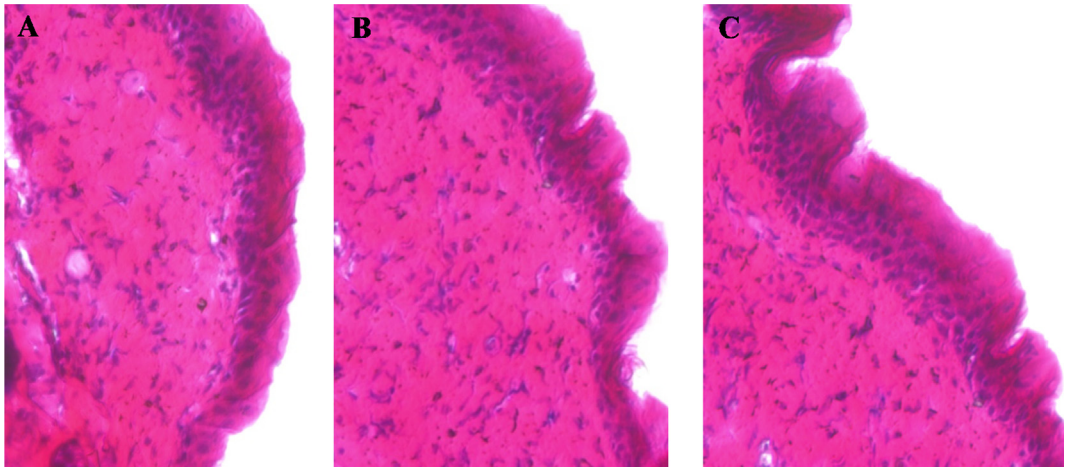

Fig. 9. In vivo histopathological evaluation of mice skin sections (×40) treated with (A) D-PBS, (B) F1, and (C) [Ch][Gly]–EtOH–H_2O (15:35:50 wt%) ternary system.

was used alone, the cell viability deceased to 56%, but it was < 30% for [C1mim][DMP], which indicated that [Ch][Gly] was safer and less irritating to skin compared with [C1mim][DMP]. The results were in a good agreement with published reports in which choline-based ILs displayed less irritation on different cultured cell line e.g., HaCaT (Santos de Almeida et al., 2017), HEK-293 (Patinha et al., 2016), and HEK-A (Wu et al., 2019). Although ILs of ternary systems temporary interfered on skin, dissociated by the interaction of water at dermal region and diminished the toxicity. This can be attributed due to the biocompatible sources of the cation and anion of [Ch][Gly]. As [Ch][Gly] was completely composed of renewable biomaterials and being GRAS in nature, the disintegrated acids-bases didn't execute considerable irritation on tissue (Wu et al., 2019). Therefore, the IL-based ternary systems can be considered a potential TDDSs.

3.11. *In vivo histological study*

In vivo histological study was performed to assess the safety profile of the [Ch][Gly]–EtOH–IPM system (Fig. 9). The structures of the sc, epidermis, and dermis of the skin were clearly visible and organized after treatment with the F1 and [Ch][Gly]–EtOH–H_2O systems (Fig. 9B and C), similar to the control (D-PBS) (Fig. 9**A**). Conversely, when the skin was treated with the [Bmim][Cl]–EtOH–H_2O (15:35:50 wt%) system, all of three mice in this group were died after 12 h, which confirmed the toxicity of imidazolium-based ILs. Therefore, the ILs used in this study had no adverse effect on the skin when the IL-based ternary systems were used for transdermal delivery of a sparingly soluble drug.

4. Conclusion

Potent ternary systems with high solubilization capacity for the sparingly soluble drug ACV have been developed by combining biocompatible IL, EtOH, and IPM. The presence of IPM as a lipophilic phase and EtOH as a co-solvent were mainly responsible for formation of thermodynamically stable IL-based ternary systems. ACV permeation from the IL–EtOH–IPM ternary systems into and across YMP skin was found to be significantly enhanced owing to multiple factors, such the high ACV solubility in the IL, IL–EtOH, and IL–EtOH–IPM, the push–pull effect of lipophilic IPM and amphiphilic EtOH, and the synergistic penetration enhancing effect of the components. In addition, the presence of the IL in the IL-based ternary systems reduced the skin barrier properties by disturbing the regularly ordered arrangements of corneocytes and the sc. In vitro cytotoxicity against fibroblast cells (L-929) confirmed the biocompatibility of the ILs compared with commercially available ILs ([Bmim][Cl] and [C1mim][DMP]). Skin irritation tests using a reconstructed human epidermis model (LabCyte EPI-MODEL) confirmed that the proposed IL–EtOH–IPM ternary systems were safe and non-toxic as TDDSs. Furthermore, no significant changes were observed in the structures of the sc, epidermis, and dermis from histological analysis of mice skin. Therefore, ternary systems containing biocompatible ILs are promising for transdermal delivery of insoluble or sparingly soluble drugs.

Credit authorship contribution statement

Md. Rafiqul Islam: Data curation, Writing - original draft. **Md. Raihan Chowdhury:** Methodology, Writing - review & editing. **Rie Wakabayashi:** Writing - review & editing. **Yoshiro Tahara:** Writing - review & editing. **Noriho Kamiya:** Writing - review & editing. **Muhammad Moniruzzaman:** Conceptualization, Writing - review & editing. **Masahiro Goto:** Supervision, Writing - review & editing.

Declaration of Competing Interest

The authors declare that they have no known competing financial interests or personal relationships that could have appeared to influence the work reported in this paper.

Acknowledgments

This study was supported by the Japan Society for the Promotion of Science (JSPS) (KAKENHI No. JP20K20440). M. R. Islam thanks the Government of Japan (MEXT) for providing the scholarship to carry out higher study and research at Kyushu University. We thank Dr. M. Watanabe and Prof. Y. Hirano for providing NMR and elemental analysis facilities, respectively. We also thank Tim Cooper, PhD, from Edanz Group (www.edanzediting.com/ac) for editing a draft of this manuscript.

Appendix A. Supplementary material

Supplementary data to this article can be found online at https://doi.org/10.1016/j.ijpharm.2020.119335.

References

Abe, M., Kuroda, K., Sato, D., Kunimura, H., Ohno, H., 2015. Effects of polarity, hydrophobicity, and density of ionic liquids on cellulose solubility. Phys. Chem. Chem. Phys. 17, 32276–32282. https://doi.org/10.1039/c5cp05808b.
Adawiyah, N., Moniruzzaman, M., Hawatulaila, S., Goto, M., 2016. Ionic liquids as a

potential tool for drug delivery systems. Medchemcomm 7, 1881–1897. https://doi.org/10.1039/c6md00358c.
Ali, M.K., Moshikur, R.M., Wakabayashi, R., Tahara, Y., Moniruzzaman, M., Kamiya, N., Goto, M., 2019. Synthesis and characterization of choline–fatty-acid-based ionic liquids: A new biocompatible surfactant. J. Colloid Interf. Sci. 551, 72–80. https://doi.org/10.1016/j.jcis.2019.04.095.
Amde, M., Liu, J.F., Pang, L., 2015. Environmental application, fate, effects, and concerns of ionic liquids: a review. Environ. Sci. Technol. 49, 12611–12627. https://doi.org/10.1021/acs.est.5b03123.
Amjadi, M., Sheykhansari, S., Nelson, B.J., Sitti, M., 2018. Recent advances in wearable transdermal delivery systems. Adv. Mater. 30, 1–19. https://doi.org/10.1002/adma.201704530.
Arora, A., Kisak, E., Karande, P., Newsam, J., Mitragotri, S., 2010. Multicomponent chemical enhancer formulations for transdermal drug delivery: more is not always better. J. Control. Release 144, 175–180. https://doi.org/10.1016/j.jconrel.2010.02.015.
Carter, P., Narasimhan, B., Wang, Q., 2019. Biocompatible nanoparticles and vesicular systems in transdermal drug delivery for various skin diseases. Int. J. Pharm. 555, 49–62. https://doi.org/10.1016/j.ijpharm.2018.11.032.
Chen, Y., Quan, P., Liu, X., Wang, M., Fang, L., 2014. Novel chemical permeation enhancers for transdermal drug delivery. Asian J. Pharm. Sci. 9, 51–64. https://doi.org/10.1016/j.ajps.2014.01.001.
Chen, Z., Lv, Y., Qi, J., Zhu, Q., Lu, Y., Wu, W., 2018. Overcoming or circumventing the stratum corneum barrier for efficient transcutaneous immunization. Drug Discov. Today 23, 181–186. https://doi.org/10.1016/j.drudis.2017.09.017.
Chowdhury, M.R., Moshikur, R.M., Wakabayashi, R., Tahara, Y., Kamiya, N., Moniruzzaman, M., Goto, M., 2019a. Development of a novel ionic liquid-curcumin complex to enhance its solubility, stability, and activity. Chem. Commun. 55, 7737–7740. https://doi.org/10.1039/c9cc02812a.
Chowdhury, M.R., Moshikur, R.M., Wakabayashi, R., Tahara, Y., Kamiya, N., Moniruzzaman, M., Goto, M., 2019b. In vivo biocompatibility, pharmacokinetics, antitumor efficacy, and hypersensitivity evaluation of ionic liquid-mediated paclitaxel formulations. Int. J. Pharm. 565, 219–226. https://doi.org/10.1016/j.ijpharm.2019.05.020.
Chowdhury, M.R., Moshikur, R.M., Wakabayashi, R., Tahara, Y., Kamiya, N., Moniruzzaman, M., Goto, M., 2018. Ionic-Liquid-based paclitaxel preparation: a new potential formulation for cancer treatment. Mol. Pharm. 15, 2484–2488. https://doi.org/10.1021/acs.molpharmaceut.8b00305.
Constable, D.J.C., Jimenez-Gonzalez, C., Henderson, R.K., 2007. Perspective on solvent use in the pharmaceutical industry. Org. Process Res. Dev. 11, 133–137. https://doi.org/10.1021/op060170h.
De Santis, S., Masci, G., Casciotta, F., Caminiti, R., Scarpellini, E., Campetella, M., Gontrani, L., 2015. Cholinium-amino acid based ionic liquids: a new method of synthesis and physico-chemical characterization. Phys. Chem. Chem. Phys. 17, 20687–20698. https://doi.org/10.1039/c5cp01612f.
Eichner, A., Stahlberg, S., Sonnenberger, S., Lange, S., Dobner, B., Ostermann, A., Schrader, T.E., Hauß, T., Schroeter, A., Huster, D., Neubert, R.H.H., 2017. Influence of the penetration enhancer isopropyl myristate on stratum corneum lipid model membranes revealed by neutron diffraction and 2H NMR experiments. Biochim. Biophys. Acta - Biomembr. 1859, 745–755. https://doi.org/10.1016/j.bbamem.2017.01.029.
Fukaya, Y., Sugimoto, A., Ohno, H., 2006. Superior solubility of polysaccharides in low viscosity, polar and halogen-free 1,3-dialkylimidazolium formates. Biomacromolecules 7, 3295–3297. https://doi.org/10.1021/bm060327d.
Gomes, J.M., Silva, S.S., Reis, R.L., 2019. Biocompatible ionic liquids: Fundamental behaviours and applications. Chem. Soc. Rev. 48, 4317–4335. https://doi.org/10.1039/c9cs00016j.
Gouveia, W., Jorge, T.F., Martins, S., Meireles, M., Carolino, M., Cruz, C., Almeida, T.V., Araújo, M.E.M., 2014. Toxicity of ionic liquids prepared from biomaterials. Chemosphere 104, 51–56. https://doi.org/10.1016/j.chemosphere.2013.10.055.
Gupta, R., Dwadasi, B.S., Rai, B., Mitragotri, S., 2019. Effect of chemical permeation enhancers on skin permeability: in silico screening using molecular dynamics simulations. Sci. Rep. 9, 1–11. https://doi.org/10.1038/s41598-018-37900-0.
Hou, X.D., Liu, Q.P., Smith, T.J., Li, N., Zong, M.H., 2013. Evaluation of toxicity and biodegradability of cholinium amino acids ionic liquids. PLoS One 8, e59145. https://doi.org/10.1371/journal.pone.0059145.
Huang, W., Wu, X., Qi, J., Zhu, Q., Wu, W., Lu, Y., Chen, Z., 2019. Ionic liquids: green and tailor-made solvents in drug delivery. Drug Discov. Today 00, 1–8. https://doi.org/10.1016/j.drudis.2019.09.018.
Karande, P., Mitragotri, S., 2009. Enhancement of transdermal drug delivery via synergistic action of chemicals. Biochim. Biophys. Acta - Biomembr. 1788, 2362–2373. https://doi.org/10.1016/j.bbamem.2009.08.015.
Kim, Y.C., Park, J.H., Ludovice, P.J., Prausnitz, M.R., 2008. Synergistic enhancement of skin permeability by N-lauroylsarcosine and ethanol. Int. J. Pharm. 352, 129–138. https://doi.org/10.1016/j.ijpharm.2007.10.031.
Kumar, S., Zakrewsky, M., Chen, M., Menegatti, S., Muraski, J.A., Mitragotri, S., 2015. Peptides as skin penetration enhancers: Mechanisms of action. J. Control. Release 199, 168–178. https://doi.org/10.1016/j.jconrel.2014.12.006.
Lane, M.E., 2013. Skin penetration enhancers. Int. J. Pharm. 447, 12–21. https://doi.org/10.1016/j.ijpharm.2013.02.040.
Liu, P., Cettina, M., Wong, J., 2009. Effects of isopropanol-isopropyl myristate binary enhancers on in vitro transport of estradiol in human epidermis: a mechanistic evaluation. J. Pharm. Sci. 98, 565–572. https://doi.org/10.1002/jps.
Lotfi, M., Moniruzzaman, M., Sivapragasam, M., Kandasamy, S., Abdul Mutalib, M.I., Alitheen, N.B., Goto, M., 2017. Solubility of acyclovir in nontoxic and biodegradable ionic liquids: COSMO-RS prediction and experimental verification. J. Mol. Liq. 243, 124–131. https://doi.org/10.1016/j.molliq.2017.08.020.
Moniruzzaman, M., Kamiya, N., Goto, M., 2010a. Ionic liquid based microemulsion with pharmaceutically accepted components: formulation and potential applications. J. Colloid Interf. Sci. 352, 136–142. https://doi.org/10.1016/j.jcis.2010.08.035.
Moniruzzaman, M., Tamura, M., Tahara, Y., Kamiya, N., Goto, M., 2010b. Ionic liquid-in-oil microemulsion as a potential carrier of sparingly soluble drug: characterization and cytotoxicity evaluation. Int. J. Pharm. 400, 243–250. https://doi.org/10.1016/j.ijpharm.2010.08.034.
Monti, D., Egiziano, E., Burgalassi, S., Chetoni, P., Chiappe, C., Sanzone, A., Tampucci, S., 2017. Ionic liquids as potential enhancers for transdermal drug delivery. Int. J. Pharm. 516, 45–51.
Moshikur, R.M., Chowdhury, M.R., Wakabayashi, R., Tahara, Y., Moniruzzaman, M., Goto, M., 2018. Characterization and cytotoxicity evaluation of biocompatible amino acid esters used to convert salicylic acid into ionic liquids. Int. J. Pharm. 546, 31–38. https://doi.org/10.1016/j.ijpharm.2018.05.021.
Muhammad, N., Man, Z.B., Bustam, M.A., Mutalib, M.I.A., Wilfred, C.D., Ra, S., 2011. Synthesis and thermophysical properties of low viscosity amino acid-based ionic liquids. J. Chem. Eng. Data 56, 3157–3162.
Nurunnabi, M., Ibsen, K.N., Tanner, E.E.L., Mitragotri, S., 2019. Oral ionic liquid for the treatment of diet-induced obesity. Proc. Natl. Acad. Sci. U. S. A. 116, 25042–25047. https://doi.org/10.1073/pnas.1914426116.
Panchagnula, R., Desu, H., Jain, A., Khandavilli, S., 2005. Feasibility studies of dermal delivery of paclitaxel with binary combinations of ethanol and isopropyl myristate: Role of solubility, partitioning and lipid bilayer perturbation. Farmaco 60, 894–899. https://doi.org/10.1016/j.farmac.2005.07.004.
Patinha, D.J.S., Tomé, L.C., Florindo, C., Soares, H.R., Coroadinha, A.S., Marrucho, I.M., 2016. New low-toxicity cholinium-based ionic liquids with perfluoroalkanoate anions for aqueous biphasic system implementation. ACS Sustain. Chem. Eng. 4, 2670–2679. https://doi.org/10.1021/acssuschemeng.6b00171.
Piao, H., Kamiya, N., Hirata, A., Fujii, T., Goto, M., 2008. A novel solid-in-oil nanosuspension for transdermal delivery of diclofenac sodium. Pharm. Res. 25, 896–901. https://doi.org/10.1007/s11095-007-9445-7.
Pramanick, S., Singodia, D., Chandel, V., 2013. Excipient selection in parenteral formulation development. Pharma Times 45, 65–77.
Prausnitz, M.R., Langer, R., 2008. Microneedles- Transdermal drug delivery. Nat. Biotechnol. 26, 1261–1268. https://doi.org/10.1038/nbt.1504.
Roger, R.D., Seddon, K.R., 2003. Ionic liquids-solvents of the future? Science (80-.) 302, 792–793. https://doi.org/10.1126/science.1090313.
Saffari, M., Shirazi, F.H., Moghimi, H.R., 2016. Terpene-loaded liposomes and isopropyl myristate as chemical permeation enhancers toward liposomal gene delivery in lung cancer cells; a comparative study. Iran. J. Pharm. Res. 15, 261–267. https://doi.org/10.22037/ijpr.2016.1884.
Santos de Almeida, T., Júlio, A., Saraiva, N., Fernandes, A.S., Araújo, M.E.M., Baby, A.R., Rosado, C., Mota, J.P., 2017. Choline- versus imidazole-based ionic liquids as functional ingredients in topical delivery systems: cytotoxicity, solubility, and skin permeation studies. Drug Dev. Ind. Pharm. 43, 1858–1865. https://doi.org/10.1080/03639045.2017.1349788.
Schwarz, J.C., Pagitsch, E., Valenta, C., 2013. Comparison of ATR-FTIR spectra of porcine vaginal and buccal mucosa with ear skin and penetration analysis of drug and vehicle components into pig ear. Eur. J. Pharm. Sci. 50, 595–600. https://doi.org/10.1016/j.ejps.2012.12.020.
Shah, D.K., Khandavilli, S., Panchagnula, R., 2008. Alteration of skin hydration and its barrier function by vehicle and permeation enhancers: a study using TGA, FTIR, TEWL and drug permeation as markers. Methods Find. Exp. Clin. Pharmacol. 30, 499–512. https://doi.org/10.1358/mf.2008.30.7.1159653.
Sidat, Z., Marimuthu, T., Kumar, P., Toit, L.C., Kondiah, P.P.D., Choonara, Y.E., Pillay, V., 2019. Ionic liquids as potential and synergistic permeation enhancers for transdermal drug delivery. Pharmaceutics 11, 96. https://doi.org/10.3390/pharmaceutics11020096.
Sintov, A.C., Shapiro, L., 2004. New microemulsion vehicle facilitates percutaneous penetration in vitro and cutaneous drug bioavailability in vivo. J. Control. Release 95, 173–183. https://doi.org/10.1016/j.jconrel.2003.11.004.
Sivapragasam, M., Moniruzzaman, M., Goto, M., 2019. An overview on the toxicological properties of ionic liquids toward microorganisms. Biotechnol. J. 1900073, 1–9. https://doi.org/10.1002/biot.201900073.
Strickley, R.G., 2004. Solubilizing excipients in oral and injectable formulations. Pharm. Res. 21, 201–230. https://doi.org/10.1023/B:PHAM.0000016235.32639.23.
Summerfield, A., Meurens, F., Ricklin, M.E., 2015. The immunology of the porcine skin and its value as a model for human skin. Mol. Immunol. 66, 14–21. https://doi.org/10.1016/j.molimm.2014.10.023.
Szumała, P., Jungnickel, C., Kozłowska-Tylingo, K., Jacyna, B., Cal, K., 2019. Transdermal transport of collagen and hyaluronic acid using water in oil microemulsion. Int. J. Pharm. 572. https://doi.org/10.1016/j.ijpharm.2019.118738.
Tahara, Y., Honda, S., Kamiya, N., Piao, H., Hirata, A., Hayakawa, E., Fujii, T., Goto, M., 2008. A solid-in-oil nanodispersion for transcutaneous protein delivery. J. Control. Release 131, 14–18. https://doi.org/10.1016/j.jconrel.2008.07.015.
Wang, C., Zhu, J., Zhang, D., Yang, Y., Zheng, L., Qu, Y., Yang, X., Cui, X., 2018. Ionic liquid – microemulsions assisting in the transdermal delivery of dencichine: preparation, in-vitro and in-vivo evaluations, and investigation of the permeation mechanism. Int. J. Pharm. 535, 120–131. https://doi.org/10.1016/j.ijpharm.2017.10.024.
Watkinson, R.M., Herkenne, C., Guy, R.H., Hadgraft, J., Oliveira, G., Lane, M.E., 2009. Influence of ethanol on the solubility, ionization and permeation characteristics of ibuprofen in silicone and human skin. Skin Pharmacol. Physiol. 22, 15–21. https://doi.org/10.1159/000183922.
Wu, X., Chen, Z., Li, Yang, Yu, Q., Lu, Y., Zhu, Q., Li, Ying, An, D., Qi, J., Wu, W., 2019.

Improving dermal delivery of hydrophilic macromolecules by biocompatible ionic liquid based on choline and malic acid. Int. J. Pharm. 558, 380–387. https://doi.org/10.1016/j.ijpharm.2019.01.021.

Yazdani, A., Sivapragasam, M., Leveque, J.M., Moniruzzaman, M., 2016. Microbial biocompatibility and biodegradability of choline-amino acid based ionic liquids. J. Microb. Biochem. Technol. 08, 415–421. https://doi.org/10.4172/1948-5948.1000318.

Zeisel, S.H., Da Costa, K.A., 2009. Choline: An essential nutrient for public health. Nutr. Rev. 67, 615–623. https://doi.org/10.1111/j.1753-4887.2009.00246.x.

Zheng, L., Zhao, Z., Yang, Y., Li, Y., Wang, C., 2020. Novel skin permeation enhancers based on amino acid ester ionic liquid: Design and permeation mechanism. Int. J. Pharm. 576, 119031. https://doi.org/10.1016/j.ijpharm.2020.119031.

Zidan, A.S., Kamal, N., Alayoubi, A., Seggel, M., Ibrahim, S., Rahman, Z., Cruz, C.N., Ashraf, M., 2017. Effect of isopropyl myristate on transdermal permeation of testosterone from carbopol gel. J. Pharm. Sci. 106, 1805–1813. https://doi.org/10.1016/j.xphs.2017.03.016.